Short Papers

Harvesting-Throughput Tradeoff for CDMA-Based Underlay Cognitive Radio Networks With Wireless Energy Harvesting

Meng Zheng, Wei Liang, and Haibin Yu

***Abstract*—This paper considers a green cognitive radio network wherein each secondary user (SU) is solely powered by an energy harvester which extracts energy from RF signals of a primary user transmitter. Each SU operates in a harvesting–transmitting fashion periodically. In each period, all SUs first harvest energy for a fixed duration and then transmit data using the harvested energy to one access point for the rest of the period in the code-division multiple access method. Considering the intrinsic harvesting-throughput tradeoff, we jointly optimize the harvesting time and transmit powers of SUs to maximize the sum throughput of the network, subject to the primary interference constraint and the energy causality constraint. Despite of the nonconvex nature of the formulated optimization problem, we find an equivalent but convex substitution to the original problem. Then, we propose a dual-decomposition-based solution method to solve the problem. Simulations finally demonstrate the efficiency of this paper.**

***Index Terms*—Cognitive radio, energy causality, harvesting-throughput tradeoff, underlay, wireless energy harvesting.**

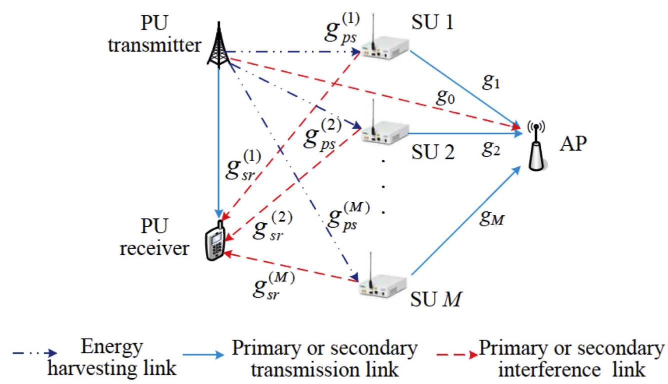

Fig. 1. System model.

I. Introduction

Energy harvesting is a promising solution to the energy-constrained problem for wireless networks as it can provide perpetual energy supply without battery recharging or replacement. In particular, radio frequency (RF) energy harvesting becomes more flexible and sustainable than solar or wind energy harvesting, since the RF signals radiated by ambient transmitters are consistently available [1]–[3]. Magnetic induction energy harvesting is another promising technology which harvests the electromagnetic energy around hight voltage power lines. However, it is only available in certain environments (e.g., power grid). In this paper, we are interested in RF-powered cognitive radio networks (RF-CRNs) and study a green coexistence paradigm for RF-CRNs.

According to the coexistence paradigm, the existing works on RF-CRNs can be classified into three categories, namely, interweave, overlay, and underlay. In the interweave paradigm, secondary users (SUs) first harvest energy and then opportunistically access the licensed spectrum when primary users (PUs) are detected as inactive [4]–[7]. In the overlay paradigm, SUs use the harvested energy from the PU signal to forward the data of both PUs and SUs, provided that perfect cooperations between PUs and SUs [8]–[10] are assumed. In the underlay paradigm, SUs harvest energy from the RF signal of PUs or other SUs, and transmit with the harvested energy provided the interference to PUs is below a tolerable threshold [11]–[12].

This paper studies an underlay RF-CRN that works in a "harvest-then-transmit" fashion, i.e., SUs first harvest energy from RF signals of one PU and then transmit data using the harvested energy to one access point (AP) in the code-division multiple access (CDMA) method. Considering the primary interference constraint and the energy causality constraint, we formulate a throughput maximization problem for RF-CRNs in terms of harvesting time and transmit powers. Moreover, we propose a dual-decomposition-based solution method to solve the formulated problem. Finally, we employ simulations to analyze the throughput performance of the studied RF-CRN under different scenarios and demonstrate the throughput improvement of this paper over TDMA-based RF-CRNs. The main contributions of this paper can be summarized as follows.

1) This paper for the first time studies the harvesting-throughput tradeoff for CDMA-based underlay RF-CRNs by formulating a throughput maximization problem.
2) Despite the global coupling of harvesting time and transmit powers, we prove that the formulated optimization problem for RF-CRNs can be equivalently reformulated as a convex problem.
3) We propose to solve the convex substitution via a dual-decomposition-based solution method whose convergence and global optimality are guaranteed by convex theory.

II. System Model

We consider a time-slotted RF-CRN with one PU transmitter-receiver pair, M SUs and one AP, as shown in Fig. 1. The link between each SU (the PU transmitter) and the PU receiver (the AP) is referred as the primary (secondary) interference link. The link between the

Manuscript received June 8, 2016; revised October 24, 2016; accepted December 4, 2016. Date of publication December 23, 2016; date of current version August 23, 2018. This work was supported in part by the Natural Science Foundation of China under Grant 61233007, Grant 61304263, and Grant 61673371, in part by the Liaoning Provincial Natural Science Foundation of China under Grant 2014020081, and in part by the Youth Innovation Promotion Association, Chinese Academy of Sciences, under Grant 2015157. *(Corresponding authors: Haibin Yu; Wei Liang.)*

The authors are with the State Key Laboratory of Robotics and the Key Laboratory of Networked Control Systems, Shenyang Institute of Automation, Chinese Academy of Sciences, Shenyang 110016, China (e-mail: zhengmeng_6@sia.cn; weiliang@sia.cn; yhb@sia.cn).

Digital Object Identifier 10.1109/JSYST.2016.2636278

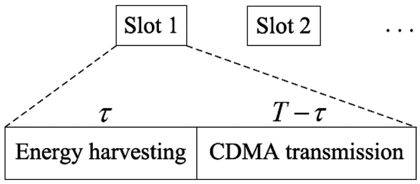

Fig. 2. Slot architecture.

PU transmitter and each SU is referred as the energy harvesting link. The link between the PU transmitter (each SU) and the PU receiver (the AP) is referred as the primary (secondary) transmission link. For notational convenience, we drop the time index and consider an arbitrary slot. The AP has a fixed power supply, whereas each SU is powered by an energy harvester which harvests green energy from RF signals of the PU transmitter. Each SU operates in a half-duplex mode, i.e., it can only harvest or transmit at one time. Therefore, a "harvest-then-transmit" fashion, which partitions one time slot with duration T into two orthogonal phases, is adopted in this paper. Fig. 2 presents the slot architecture of the RF-CRN. An example RF-CRN may be a wireless sensor network consisting of one sink and M RF-powered sensors deployed in a hostile environment, such that sensors send information to the sink and harvest energy from a coexisting PU transmitter.

Energy Harvesting Phase: Each SU is assumed with an infinite energy storage device. Let e_i denotes the initial energy of SU i at the beginning of the studied slot. In the energy harvesting phase, SU i ($i = 1, 2, \dots, M$) harvests energy for a duration τ ($0 \le \tau \le T$). The total available energy by the end of the harvesting phase is given by

$$E_i = \xi_i g_{ps}^{(i)} \tau P_t + e_i \tag{1}$$

where ξ_i ($0 < \xi_i < 1$), $g_{ps}^{(i)}$, and P_t denote the energy conversation efficiency of SU i (which depends on the hardware design of energy harvester), the energy harvesting link gain of SU i, and the transmit power of the PU transmitter, respectively.

CDMA Transmission Phase: We focus on the uplink scheme where SUs communicate with the AP, and we assume that SUs send their data in the uplink by using the CDMA method. In the CDMA transmission phase, each SU will consume the harvested energy for data transmission. However, the transmit power of the SU i (P_i) is subject to its harvested energy

$$P_i - \frac{E_i}{T-\tau} \le 0,\ i = 1, 2, \dots, M \tag{2}$$

and the primary interference constraint imposed by the PU receiver

$$\sum_{i=1}^{M} g_{sr}^{(i)} P_i \le I_p \tag{3}$$

where I_p denotes the peak interference power that the PU receiver can tolerate and $g_{sr}^{(i)}$ denotes the primary interference link gain between the PU receiver and SU i. Equation (2) is referred as the energy causality constraint [11].

Network Throughput: Due to the strictly limited transmit power and multiple-access interference, the throughput performance of the RF-CRN is very poor. To improve the throughput, we use the successive interference canceler detector (SICD) [13] with predefined decoding order at the AP. With the SICD technique, the AP decodes SU signals in sequence. For notational convenience, we order SU i as the i-th SU. Once the i-th SU is decoded, the reconstructed signal for SU i is removed from the composite signal. The process continues until all SUs are decoded. We assume perfect cancellation in SICD as we are interested in obtaining a throughput upper bound for practical systems. The effects of cancellation error will be studied in our future work. Then, we can calculate the maximum achievable data rate per hertz for SU i as follows:

$$R_i = \log\left(1 + \frac{g_i P_i}{\sum_{k=i+1}^{M} g_k P_k + g_0 P_t + \sigma^2}\right) \tag{4}$$

where g_i ($i = 1, 2, \dots, M$) is the secondary transmission link gain between SU i and the AP, and g_0 is the primary interference channel gain between the PU transmitter and the AP. Moreover, σ^2 is the noise variance at the receiver of the AP.

Subsequently, we obtain the average throughput of the RF-CRN which is given as follows:

$$f(\tau, \mathbf{P}) = \frac{T-\tau}{T} \sum_{i=1}^{M} R_i \tag{5}$$

where $\mathbf{P} = (P_1, P_2, \dots, P_M)$ denotes the power vector of SUs.

Finally, we arrive at the throughput maximization problem for the RF-CRN in terms of the harvesting time and transmit powers

$$\max_{\tau, \mathbf{P}}\ f(\tau, \mathbf{P}) \tag{6a}$$

$$\text{s.t. } (2) \text{ and } (3)$$

$$\mathbf{P} \succeq 0,\ 0 \le \tau \le T \tag{6b}$$

where "$\succeq$" denotes the componentwise inequality. To focus on the throughput upper bound, this paper assumes that $\{P_t, I_p, g_{sr}^{(i)}, g_{ps}^{(i)}, g_i, g_0\}$ are perfectly known by the RF-CRN.[1]

III. Solution Method

With the SICD technology, we can rewrite $f(\tau, \mathbf{P})$ as follows:

$$\begin{aligned} f(\tau, \mathbf{P}) &= \frac{T-\tau}{T} \sum_{i=1}^{M} \log\left(1 + \frac{g_i P_i}{\sum_{k=i+1}^{M} g_k P_k + g_0 P_t + \sigma^2}\right) \\ &= \frac{T-\tau}{T} \log\left(\frac{\sum_{i=1}^{M} g_i P_i}{g_0 P_t + \sigma^2} + 1\right). \end{aligned} \tag{7}$$

Further, using the monotonicity property of logarithm function, we reformulate problem (8) as follows:

$$\max_{\tau, \mathbf{P}}\ F(\tau, \mathbf{P})$$

$$\text{s.t. } (2),\ (3),\ \text{and } (6b) \tag{8}$$

where $F(\tau, \mathbf{P}) = F_1(\tau) + F_2(\mathbf{P})$, with $F_1(\tau) = \log\left(\frac{T-\tau}{T}\right)$, $F_2(\mathbf{P}) = \log(c(\mathbf{P}))$, and $c(\mathbf{P}) = \log(\frac{\sum_{i=1}^{M} g_i P_i}{g_0 P_t + \sigma^2} + 1)$.

Theorem 1: Problem (8) is a convex problem in τ and $\mathbf{P}$.

Proof: The proof of Theorem 1 is given in Appendix A. ∎

[1] P_t and I_p are the public PU information. $g_{sr}^{(i)}$ can be obtained by SU i via sending pilot signals to the PU receiver and collecting channel estimation feedback from the PU receiver. $g_{ps}^{(i)}$ can be estimated based on the received PU signals by SU i. g_i can be obtained by the AP via sending pilot signals to SU i and collecting channel estimation feedback from SU i. g_0 can be estimated by the AP based on the received PU signals.

In addition to the convexity of problem (8), we can trivially verify that the slater's condition [14] for problem (8) holds. Therefore, we can achieve the optimal solution to problem (8) by solving its dual problem.

We first relax (2) and (3) and then form the Lagrangian dual function and the dual problem of problem (8)

$$D(\lambda, \mu) = \max_{(\tau, \mathbf{P}) \in (6b)} L(\lambda, \mu, \tau, \mathbf{P}) \quad (9)$$

where $L(\lambda, \mu, \tau, \mathbf{P}) = F(\tau, \mathbf{P}) - \sum_{i=1}^{M} \lambda_i (P_i - \frac{\xi_i g_{ps}^{(i)} \tau P_t + e_i}{T-\tau}) - \mu(\sum_{i=1}^{M} g_{sr}^{(i)} P_i - I_p)$, and

$$\min_{\lambda \succeq 0, \mu \geq 0} D(\lambda, \mu). \quad (10)$$

Theorem 2: For given $\lambda \succeq 0$ and $\mu \geq 0$, the optimal harvesting time and transmit powers of problem (9), respectively, have the following closed-form relation:

$$\tau^* = \max \left\{ T - \sum_{i=1}^{M} \lambda_i \left(\xi_i g_{ps}^{(i)} P_t T + e_i \right), 0 \right\} \quad (11)$$

and

$$\sum_{i=1}^{M} g_i P_i^* = (\exp(\mathrm{W}(\Delta_i)) - 1) (g_0 P_t + \sigma^2) \quad (12)$$

where $\Delta_i = \frac{g_i}{(g_0 P_t + \sigma^2)(\lambda_i + g_{sr}^{(i)} \mu)}$ and $\mathrm{W}(.)$ denotes the Lambert W function [15].

Proof: The proof of Theorem 2 is given in Appendix B. ■

Although (12) gives the weighted sum of P^*, we have to evaluate P_i^* numerically by using the gradient decent method. Specifically, in the t-th iteration, we update $P_i(t)$ as follows:

$$P_i(t) = \max \left\{ P_i(t-1) - \alpha(t) \frac{\partial L}{\partial P_i} |_{P_i = P_i(t-1)}, 0 \right\}, \quad (13)$$

where $\alpha(t)$ represents the step-size in the t-th iteration.

Next, we compute the optimal dual variables λ and μ that minimize $D(\lambda, \mu)$ by using the subgradient-projection method. Specifically, the subgradients of $D(\lambda, \mu)$ at λ_i and μ are calculated as

$$\partial_{\lambda_i} D = - \left(P_i - \frac{\xi_i g_{ps}^{(i)} \tau P_t + e_i}{T - \tau} \right) \quad (14)$$

$$\partial_{\mu} D = - \left(\sum_{i=1}^{M} g_{sr}^{(i)} P_i - I_p \right) \quad (15)$$

and in the n-th iteration, we update λ_i and μ as follows:

$$\lambda_i(n) = \max \{ \lambda_i(n-1) + \beta(n) \partial_{\lambda_i} D(n-1), 0 \} \quad (16)$$

$$\mu(n) = \max \{ \mu(n-1) + \beta(n) \partial_{\mu} D(n-1), 0 \} \quad (17)$$

where $\beta(n)$ denotes the step-size in the n-th iteration.

The above dual-decomposition solution method to problem (8) is summarized in Algorithm 1. The outer loop and the inner loop of Algorithm 1 correspond to the subgradient projection method (16)–(17) and the gradient decent method (13), respectively, both of which converge linearly to their optimum if $\alpha(t)$ and $\beta(n)$ are properly selected according to convex optimization theory [14]. Due to τ^* in (11) and $\partial_{\mu} D$ in (15), both of which contain global information, Algorithm 1 is a centralized algorithm that has to be offline implemented in the AP.

Algorithm 1: the Dual-decomposition-based solution method.

Input: $\epsilon > 0$, $\lambda(0)$, $\mu(0)$, $t = 0$, $n = 0$, P_t, I_p, σ^2, T, α, $\beta(n) = \frac{1}{n}$, g_0, e_i, ξ_i, $g_{ps}^{(i)}$, $g_{sr}^{(i)}$, g_i, $i = 1, 2, \ldots, M$.

1: **repeat**

2: $n = n + 1$; Calculate $\tau^*(n)$ according to (11).

3: **repeat**

4: $t = t + 1$; Calculate the gradient information $\frac{\partial L}{\partial P_i} |_{P_i = P_i(t-1)}$ and update $P_i(t)$ according to (13).

5: **until** $L(\tau^*(n), \mathbf{P}(t)) - L(\tau^*(n), \mathbf{P}(t-1)) < \epsilon$.

6: $\mathbf{P}^*(n) = \mathbf{P}(t)$.

7: Calculate the subgradient information $\partial_{\lambda_i} D$ and $\partial_{\mu} D$ according to (14) and (15), respectively, and update $\lambda_i(n)$ and $\mu(n)$ according to (16) and (17), respectively.

8: **until** $D(\lambda(n), \mu(n)) - D(\lambda(n-1), \mu(n-1)) < \epsilon$.

Output: $\left(\hat{\tau}, \hat{\mathbf{P}}\right) = (\tau^*(n), \mathbf{P}^*(n))$ and $\hat{f} = D(\lambda(n), \mu(n))$.

IV. Numerical Results

Numerical results are shown to validate the performance of this paper. All network parameters are selected to describe typical underlay RF-CRNs scenarios [11]–[12]. Specifically, $M = 5$, $\xi_i = 0.95$, $g_0 = 0.25$, $\sigma^2 = 1$, $e_i = 0$, $T = 0.1$ s. As the distribution of harvested energy and interference in the RF-CRN depends on the SUs locations, we assume that $g_{ps}^{(i)}$, $g_{sr}^{(i)}$, and g_i are uniformly distributed in $[0, 1]$. Numerical results are generated based on the method of batch means with 100 simulation runs for the confidence level of 95%.

Fig. 3(a) analyzes the throughput of the RF-CRN under different values of P_t and I_p, where both P_t and I_p are normalized by σ^2. It is obvious in Fig. 3(a) that $f(\tau, \mathbf{P})$ increases with the increase of I_p, which stems from the fact that increasing I_p enlarges the feasible domain of $\mathbf{P}$ and further boosts $f(\tau, \mathbf{P})$ in (7). In contrast, $f(\tau, \mathbf{P})$ is generally not monotonic in P_t. For $I_p = 3$ dB and $I_p = 4$ dB, $f(\tau, \mathbf{P})$ first increases then decreases with the increase of P_t. This is an interesting observation which can be explained as follows: on one hand, large P_t implies more harvested energy, but also more interference to the AP on the other hand. If P_t is sufficiently small (or constraint (3) is not tight), the benefit of increasing P_t outweighes its negative impact; otherwise, the increase of P_t does not enhance the transmit powers of SUs but only produces large interference to the AP.

Fig. 3(b) compares the CDMA-based RF-CRN (denoted as "CDMA") with the TDMA-based RF-CRN [11] (denoted as "TDMA") in terms of network throughput. For fair comparison, we assume that "CDMA" and "TDMA" share the same network parameters and the same slot architecture as shown in Fig. 2. Specifically, for TDMA-based RF-CRNs, we solve the following optimization problem by MATLAB:

$$\max_{\tau, \mathbf{P}} \frac{T - \tau}{MT} \sum_{i=1}^{M} \log \left(\frac{g_i P_i}{g_0 P_t + \sigma^2} + 1 \right)$$

$$\text{s.t. } (6b),\ P_i \leq \frac{M E_i}{T - \tau},\ g_{sr}^{(i)} P_i \leq I_p,\ i = 1, 2, \ldots, M.$$

Notice that the transmission phase of "TDMA" is further divided into M mini slots [11]. For an arbitrarily selected $I_P = 4$ dB, we vary the number of SUs M from 1 to 5. It is clearly shown in Fig. 3(b) that all the curves are monotonic increasing in M and moreover, "CDMA" always dominates "TDMA" for different values of M.

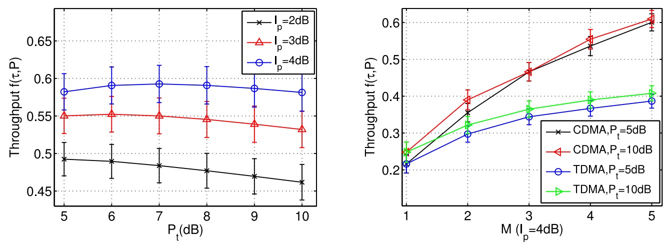

(a) (b)

Fig. 3. Throughput as a function of: (a) the transmit power of the PU transmitter P_t and (b) the number of SUs M. (a) Throughput analysis. (b) Throughput comparison.

V. Conclusion

This paper studied an underlay RF-CRN wherein each SU operates in a "harvest-then-transmit" fashion. Considering the primary interference constraint and the energy causality constraint, we jointly optimized the harvesting time and transmit powers of SUs to maximize the throughput of the RF-CRN. In order to solve the nonconvex throughput maximization problem, we first found an equivalent but convex substitution to the original problem and then proposed a dual-decomposition-based solution method to the convex substitution. Simulations analyzed the throughput performance of the RF-CRN under different scenarios and demonstrated the throughput improvement of this paper over the TDMA-based RF-CRN.

This paper can be generalized to the network setting of multiple primary sessions by imposing multiple primary interference constraints (3) and adding multiple interference terms in (7). Relevant results in [11] will be useful for the extension of this paper to the multi-hop topology.

Appendix A
Proof of Theorem 1

Proof. It is trivial to verify that $f_i(\tau, P_i) = P_i - \frac{E_i}{T-\tau}$ is jointly convex in P_i and τ. Moreover, (3) is an affine constraint of $\mathbf{P}$. Therefore, the feasible domain of problem (8) is convex since the intersection of convex sets is also convex.

Next, we prove the concavity of $F(\tau, \mathbf{P})$. It is obvious that τ and $\mathbf{P}$ are decoupled in $F(\tau, \mathbf{P})$. As $F_1(\tau)$ is strictly concave in τ, we can declare the concavity of $F(\tau, \mathbf{P})$ if $F_2(\mathbf{P})$ is concave in $\mathbf{P}$. As $F_2(\mathbf{P})$ is the logarithm function of a concave function $c(\mathbf{P})$ which is twice differentiable and positive for $\mathbf{P} \succeq 0$, we calculate the Hessian matrix of $F_2(\mathbf{P})$

$$\nabla^2 F_2(\mathbf{P}) = \frac{1}{c(\mathbf{P})}\nabla^2 c(\mathbf{P}) - \frac{1}{c^2(\mathbf{P})}\nabla c(\mathbf{P})\nabla c(\mathbf{P})^T. \tag{18}$$

For any $\mathbf{P} \succeq 0$, we have

$$\begin{aligned}\mathbf{P}^T\nabla^2 F_2(\mathbf{P})\mathbf{P} &= \frac{\mathbf{P}^T\nabla^2 c(\mathbf{P})\mathbf{P}}{c(\mathbf{P})} - \frac{\mathbf{P}^T\nabla c(\mathbf{P})\nabla c(\mathbf{P})^T\mathbf{P}}{c^2(\mathbf{P})}\\ &\leq \frac{\mathbf{P}^T\nabla^2 c(\mathbf{P})\mathbf{P}}{c(\mathbf{P})} \leq 0\end{aligned}$$

which implies the negative semidefiniteness of $\nabla^2 F_2(\mathbf{P})$ and further the concavity of $F_2(\mathbf{P})$. ∎

Appendix B
Proof of Theorem 2

Proof. For given $\lambda \succeq 0$ and $\mu \geq 0$, we obtain the first order optimality condition for problem (9) by setting the partial derivative of $L(\lambda, \mu, \tau, \mathbf{P})$ with respect to τ and P_i $(i = 1, 2, \ldots, M)$ as 0

$$\frac{\partial L}{\partial \tau} = \frac{-1}{T-\tau} + \frac{\sum_{i=1}^{M}\lambda_i\left(\xi_i g_{ps}^{(i)} P_t T + e_i\right)}{(T-\tau)^2} = 0 \tag{19}$$

and

$$\frac{\partial L}{\partial P_i} = \frac{1}{c(\mathbf{P})}\frac{g_i}{\sum_{i=1}^{M} g_i P_i + g_0 P_t + \sigma^2} - \lambda_i - g_{sr}^{(i)}\mu = 0. \tag{20}$$

The solution to (19) can be trivially obtained as $T - \sum_{i=1}^{M} \lambda_i\left(\xi_i g_{ps}^{(i)} P_t T + e_i\right)$. Considering (6b), we arrive at (11).

Next, we invoke the Lambert W function to simplify (20). We have $c(P^*) = \mathrm{W}(\Delta_i)$ and $\sum_{i=1}^{M} g_i P_i^* = (\exp(\mathrm{W}(\Delta_i)) - 1)(g_0 P_t + \sigma^2)$. This completes the proof of Theorem 2. ∎

References

[1] I. Krikidis *et al.*, "Simultaneous wireless information and power transfer in modern communication systems," *IEEE Commun. Mag.*, vol. 52, no. 11, pp. 104–110, Nov. 2014.

[2] Z. Ding *et al.*, "Application of smart antenna technologies in simultaneous wireless information and power transfer," *IEEE Commun. Mag.*, vol. 53, no. 4, pp. 86–93, Apr. 2015.

[3] D. W. K. Ng, E. S. Lo, and R. Schober, "Multiobjective resource allocation for secure communication in cognitive radio networks with wireless information and power transfer," *IEEE Trans. Veh. Technol.*, vol. 65, no. 5, pp. 3166–3184, May 2016.

[4] W. Chung *et al.*, "Spectrum sensing optimization for energy-harvesting cognitive radio systems," *IEEE Trans. Wireless Commun.*, vol. 13, no. 5, pp. 2601–2613, May 2014.

[5] Y. Zhang *et al.*, "Power vs. spectrum 2-D sensing in energy harvesting cognitive radio networks," *IEEE Trans. Signal Process.*, vol. 63, no. 23, pp. 6200–6212, Dec. 2015.

[6] D. T. Hoang *et al.*, "Opportunistic channel access and RF energy harvesting in cognitive radio networks," *IEEE J. Sel. Areas Commun.*, vol. 32, no. 11, pp. 2039–2052, Nov. 2014.

[7] S. Yin, Z. Qu, and S. Li, "Achievable throughput optimization in energy harvesting cognitive radio systems," *IEEE J. Sel. Areas Commun.*, vol. 33, no. 3, pp. 407–422, Mar. 2015.

[8] Y. Wang *et al.*, "Optimization of relay selection and ergodic capacity in cognitive radio sensor networks with wireless energy harvesting," *Pervasive Mobile Comput.*, vol. 22, pp. 33–45, Sep. 2015.

[9] Z. Yang *et al.*, "Outage performance of cognitive relay networks with wireless information and power transfer," *IEEE Trans. Veh. Technol.*, vol. 66, no. 5, pp. 3828–3833, May 2016.

[10] Z. Wang *et al.*, "Cognitive relay networks with energy harvesting and information transfer: Design, analysis, and optimization," *IEEE Trans. Wireless Commun.*, vol. 15, no. 4, pp. 2562–2576, Apr. 2016.

[11] C. Xu *et al.*, "Outage performance of underlay multi-hop cognitive relay networks with energy harvesting," *IEEE Commun. Lett.*, vol. 20, no. 6, pp. 1148–1151, Jun. 2016.

[12] M. Zheng *et al.*, "Harvesting-throughput tradeoff for RF-powered underlay cognitive radio networks," *Electron. Lett.*, vol. 52, no. 10, pp. 881–883, May 2016.

[13] D. Tse and P. Viswanath, *Fundamentals of Wireless Communication.* New York, NY, USA: Cambridge Univ. Press, 2005.

[14] S. Boyd and L. Vandenberghe, *Convex optimization*. Cambridge, U.K.: Cambridge Univ. Press, 2004.

[15] R. M. Corless *et al.*, "On the lambert W function," *Adv. Comput. Math.*, vol. 5, no. 1, pp. 329–359, Dec. 1996.